JOURNAL OF MATERIALS SCIENCE **39** (2004) 5803–5808

Dissolution kinetics of iron in liquid zinc

M.-L. GIORGI*
École Centrale Paris, Grande Voie des Vignes, 92 295 Châtenay-Malabry cedex, France
E-mail: giorgi@lgpm.ecp.fr

P. DURIGHELLO, R. NICOLLE
IRSID, Voie Romaine, BP 30320, 57283 Maizières-lès-Metz cedex, France

J.-B. GUILLOT
École Centrale Paris, Grande Voie des Vignes, 92 295 Châtenay-Malabry cedex, France

In hot dip galvanizing, steel strip is coated by immersion in a bath of molten zinc. The principal reactions that occur at the steel/liquid zinc interface are (1) dissolution of iron and (2) nucleation and growth of intermetallic compounds. In order to improve the management of industrial galvanizing baths, it is essential to evaluate the flux of dissolved iron that diffuses into the bath from the sheet. For this purpose, a rotating disk device has been developed to study the dissolution and diffusion of iron in pure liquid zinc at the temperature usually employed in galvanizing baths (465°C). Since the dissolution reaction is controlled by diffusion under these conditions, the diffusion coefficient of iron in liquid zinc has been measured and found to be:

$$D_{\mathrm{Fe}}^{\mathrm{Zn(L)}} = (9.8 \pm 0.1) \times 10^{-10}\ \mathrm{m^2 \cdot s^{-1}}$$

Nomenclature

c_i^{∞}	concentration of metal i in the bath ($\mathrm{mol \cdot m^{-3}}$)
c_i^{sat}	saturation limit of metal i in the bath ($\mathrm{mol \cdot m^{-3}}$)
$D_{\mathrm{Fe}}^{\mathrm{Zn(L)}}$	diffusion coefficient of iron in liquid zinc ($\mathrm{m^2 \cdot s^{-1}}$)
D_L	diffusion coefficient of dissolved metal i in the liquid ($\mathrm{m^2 \cdot s^{-1}}$)
k_{tot}	overall dissolution rate constant ($\mathrm{m \cdot s^{-1}}$)
$m_{\mathrm{Fe}}^{dissolved}$	mass of iron dissolved per unit surface area ($\mathrm{g \cdot m^{-2}}$)
S	surface area of the solid specimen ($\mathrm{m^2}$)
t	contact time between the two metals (s)
t_{total}	cumulative galvanizing time for the bath (s)
V	volume of the liquid bath ($\mathrm{m^3}$)
ν	kinematic viscosity of the bath ($5 \times 10^{-7}\ \mathrm{m^2 \cdot s^{-1}}$ for Zn at 465°C [21])
ω	angular velocity ($\mathrm{s^{-1}}$)
Re	Reynolds number ($= \omega r^2/\nu$ where r is the disk radius)
Sc	Schmidt number ($=\nu/D_L$)

1. Introduction

Steel is often coated with a layer of zinc in order to protect it against corrosion. One of the most commonly used coating processes is hot dip galvanizing, frequently performed in a continuous treatment line. The steel parts or strip are immersed in a bath of molten zinc or zinc alloy. Batch treatments are generally employed for galvanizing finished parts in pure zinc, while continuous treatments are used for coiled products (strip, wire and tubing), in zinc/aluminium alloy baths [1–3]. For this reason, the present study considered baths containing less than 1 wt% Al, which are the most frequently employed.

The principal reactions that occur at the steel/liquid zinc interface are (1) dissolution of iron and (2) nucleation and growth of intermetallic compounds [1–3]. Part of the iron dissolved diffuses into the bath where it contributes to the formation of intermetallic particles about twenty microns in diameter, known as dross. The zinc bath thus typically contains 0.025 to 0.06 wt% of unwanted iron from the steel. The dross is in thermodynamic equilibrium with the liquid phase and its nature depends on the composition and the temperature of the bath (e.g., δ-$FeZn_9$ and η-$Fe_2Al_5Zn_x$ for 0.15 wt% Al, 0.04 wt% Fe, at 450°C) [3–7].

In order to facilitate the management of galvanizing baths, and in particular to limit dross formation as far as possible, it is essential to evaluate the flux of iron resulting from dissolution of the steel and diffusion into the bath. For this purpose, the main aim of the present study was to develop a rotating disk device

* Author to whom all correspondence should be addressed.

for determining the iron diffusion coefficient in liquid zinc.

The work comprised the following stages:

(1) a brief review of the literature concerning the study of dissolution of a solid metal in a liquid metal using the rotating disk technique, and Levich's approach to the solution of the diffusion equations [8];

(2) the development of an appropriate rotating disk device and definition of the experimental protocol for measuring the dissolution and diffusion of iron in liquid zinc;

(3) measurement of the dissolution constant and diffusion coefficient for iron in liquid zinc.

2. The rotating disk technique

2.1. Basic principles

The rotating disk technique is often used to study reactions between a solid metal and a liquid, particularly in the field of electrochemistry, and the solution of the diffusion equations is well known for this configuration [8].

The specimen is composed of a vertical cylinder with an inert wall. The reactions take place on the lower disk-shaped face, which is immersed in the liquid. The specimen rotates about its axis with a variable angular velocity ω.

2.2. Previous studies in the field of liquid metals

Rotating disk devices have already been used to study the dissolution of a solid metal in a liquid metal [9–15]. These empirical studies have shown that the dissolution kinetics are governed by the following law:

$$\frac{\mathrm{d}c_i^{\infty}}{\mathrm{d}t} = k_{tot}\frac{S}{V}\left(c_i^{sat} - c_i^{\infty}\right) \quad (1)$$

where the metal in the course of dissolution is designated i (the notation used here is defined above). This relation remains valid even when intermetallic compounds form in the substrate [10, 11, 13, 15]. The experimental value of k_{tot} makes it possible to determine an overall value of the dissolution rate without considering the details of the interface phenomena involved (growth of alloy layers, diffusion in the liquid and solid states).

When dissolution is controlled by diffusion of the metal i in the liquid, by solving the diffusion equations, it can be shown that the dissolution constant is described by a relation whose form depends on the Schmidt number Sc for the system concerned [8, 9]:

$$k_{tot} = 0.62 D_L^{\frac{2}{3}} \nu^{-\frac{1}{6}} \omega^{\frac{1}{2}} \quad \text{for Sc} > 1000 \quad (2)$$

$$k_{tot} = 0.554 f_{\mathrm{Sc}}^{-1} D_L^{\frac{2}{3}} \nu^{-\frac{1}{6}} \omega^{\frac{1}{2}} \quad \text{for } 4 < \mathrm{Sc} < 1000 \quad (3)$$

where f_{Sc} is a function of the Schmidt number Sc tabulated in reference [9]. Equations 2 and 3 are valid for laminar flow (i.e., for a Reynolds number Re less than 10^5 in the configuration considered [8, 9]).

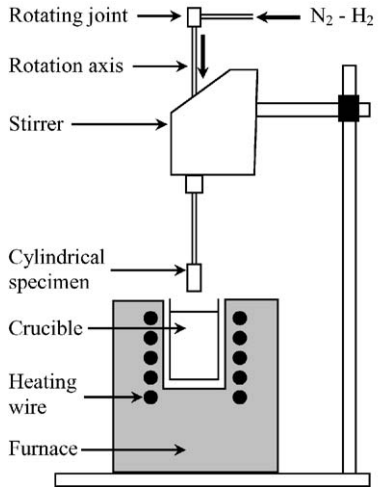

Figure 1 Schematic diagram of the rotating disk apparatus (the cylindrical specimen is composed of a disk of the steel under study, a mullite tube and a stainless steel lid fitting onto the top of the mullite tube).

Several experimental studies have demonstrated the validity of Equations 2 and 3 for initially pure liquid Al baths [10, 11, 13]. In these conditions, the intermetallic compounds formed are not stable and enhance the rate of dissolution of the metal into the liquid bath.

2.3. Experimental system

The rotating disk device comprises four main components (Fig. 1 and Table I):

- The galvanizing furnace (a muffle furnace) melts the zinc (about 6 kg contained in an alumina crucible) and maintains the required bath temperature.
- A mechanical stirrer with a digital display rotates the specimen at a precise speed, chosen within two ranges: 40 to 400 or 200 to 2000 rpm.
- The cylindrical specimen has three distinct parts: a disk of the steel under study; a mullite tube ($3Al_2O_3{\cdot}2SiO_2$) whose vertical walls remain inert in contact with the zinc bath; a stainless steel lid that fits onto the top of the mullite tube. The edge effects are negligible because the boundary layer thickness δ_0 is small compared to the disk radius [8]: δ_0 ($=3.6\ \nu^{0.5}\ \omega^{-0.5}$) varies from 3.5×10^{-4} to 7.9×10^{-4} m with the chosen rotation speeds (from 100 to 500 rpm).
- A stainless steel tube serves as the rotation axis. A notch near the bottom of the tube enables the steel disk to be attached. A rotating joint allows a N_2/H_2 (5 to 10 vol%) gas mixture to be fed onto the rotating specimen. The gas stream, with a flowrate of

TABLE I Dimensions of the rotating disk system

Component	Alumina crucible	Mullite tube	Steel specimen
Shape	Cylinder	Cylinder	Disk
Dimensions (mm)	Inside diameter: 105 Height: 110	Inside diameter: 39 Outside diameter: 45 Height: 33	Diameter: 40

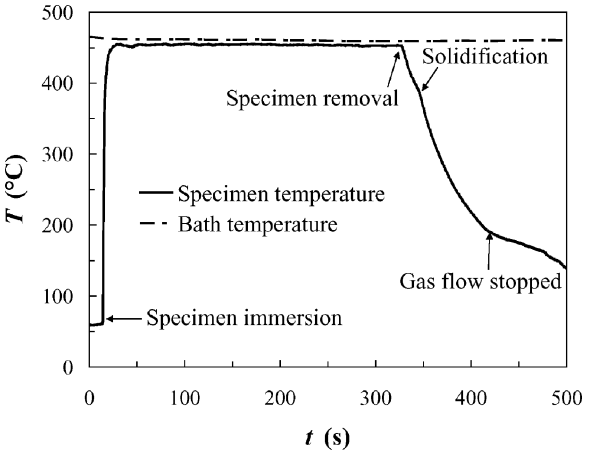

Figure 2 Specimen and bath temperature profiles (5 min galvanizing).

$1\ m^3 \cdot h^{-1}$, limits the presence of oxygen in contact with the disk specimen (to avoid oxidation).

The variation in temperature of a stationary specimen is measured with a thermocouple welded to the top face of the substrate protected by the mullite tube. The profile obtained includes several stages (Fig. 2):

- Before galvanizing, the specimen is held about 10 centimetres above the surface of the molten zinc, and is heated by radiation: its temperature rises slightly to about 60°C.
- Immersion of the specimen into the molten bath causes a rapid rise in temperature to 430°C in 5 s. The temperature of the sample is low (i.e., less than 430°C), only for a very short time compared to the galvanizing time (from 30 s to 5 min). The entry temperature is therefore believed to have a negligible effect on the data obtained. The temperature of the substrate stabilises at 454°C in 13 ± 1 s (for an initial bath temperature of 465°C).
- During galvanizing (5 min in this case), the temperature of the steel remains stable at 453 ± 3°C.
- Finally, on removal from the bath, the steel cools at $5°C \cdot s^{-1}$, the rate being enhanced by the gas flow inside the mullite tube. The temperature recording also reveals the coating solidification shelf and the interruption of the N_2/H_2 gas flow.

The temperature reached by the steel is about ten degrees less than that of the bath. However, the thermocouple measures the temperature on the top face of the disk, which is cooled by the gas. It can be assumed that the other face attains the temperature of the molten zinc. During galvanizing, because of the thermal inertia of the specimen, the bath temperature decreases slightly, by not more than 6°C for the longest immersion times (5 min).

3. Experimental protocol

3.1. Experimental material

The dissolution experiments were performed on a commercial interstitial-free steel containing titanium, designated *IF Ti*, in the form of 0.8 mm thick cold rolled strip. It represents one of the grades most commonly coated in industrial continuous galvanizing lines. The steel composition is given in Table II. The galvanizing baths were produced from ingots of pure zinc (99.995 wt%, the principal impurities being Pb, Cd, Sn, Cu) and pure aluminium (99.7 wt%, the principal impurities being Si, Cu, Pb, C).

TABLE II Composition of the *IF Ti* steel used ($\times 10^{-3}$ wt%)

C	Mn	Ti	Nb	P	S	Si	Al	Ni	Cr	Cu	N
3.3	99	56	<1	13	5	14	41	16	19	9	2.7

3.2. Galvanizing conditions

The galvanizing bath chosen contains relatively little aluminium (0.05 wt%) and only traces of iron (0.003 wt%), in order to promote the dissolution of iron [1, 16–18]. The aluminium prevents excessive oxidation of the bath surface by forming a thin film of alumina.

The temperature of the molten zinc was measured at the bottom of the crucible before and after each galvanizing treatment, and was shown to be 465 ± 4°C.

The specimen rotation speed was chosen in the range 100 to 500 rpm.

3.3. Galvanizing procedure

In order to reduce any iron oxides present on the disk surface, the latter is prepared in several steps. Ultrasonic degreasing is first of all performed in chloroform to clean off storage oils. The sheet is then pickled for 10 min in a $0.5\ mol \cdot l^{-1}$ hydrochloric acid solution containing a corrosion inhibitor ($2\ g \cdot l^{-1}\ C_6H_{12}N_4$), in order to remove oxides. Finally, it is immersed in a fluxing solution ($136\ g \cdot l^{-1}\ ZnCl_2$ and $107\ g \cdot l^{-1}\ NH_4Cl$, 50°C, 10 min) and dried (100°C, 20 min). This fluxing treatment has three beneficial effects: it completes the removal of iron oxides, subsequent oxidation is prevented by a thin film of flux, and good wetting by the molten zinc is ensured.

After this surface preparation, the specimen assembly is mounted on the rotation axis of the rotating disk device and immersed to a depth of 15 mm in the galvanizing bath before starting the rotation.

3.4. Measurement of iron dissolution from galvanized specimens

Iron dissolution is measured using a gravimetric method involving several steps: (1) weighing of the initial specimen (mass m_1); (2) pickling, fluxing, galvanizing and solidification of the coating; (3) complete dissolution of the coating in a $1\ mol \cdot l^{-1}$ hydrochloric acid solution containing a corrosion inhibitor ($4\ g \cdot l^{-1}$ of $C_6H_{12}N_4$); (4) weighing of the final specimen (mass m_2). The mass of iron dissolved per unit surface area is given by the equation:

$$m_{Fe}^{dissolved} = \frac{m_1 - m_2}{S} \quad (4)$$

Analysis of the hydrochloric acid solution by optical emission spectroscopy using an inductively coupled plasma (ICP) is used to determine the masses of iron and aluminium in the coating, $m_{Fe}^{coating}$ and $m_{Al}^{coating}$.

3.5. Analysis of the galvanizing bath

The analysis of regular samples taken from the bath after each series of six galvanized specimens, corresponding to a total immersion time of 15 min, enables the iron and aluminium contents of the bath to be monitored as a function of the total time during which the bath has been used (t_{total}).

4. Experimental results

4.1. Iron matter balance for a given rotation speed

Fig. 3 shows the variation of three parameters with specimen immersion time in the zinc bath, for extreme rotation speeds of 100 and 500 rpm:

- $m_{Fe}^{dissolved}$, total mass of iron dissolved per unit surface area;
- $m_{Fe}^{coating}$, mass of iron in the coating per unit surface area;
- $m_{Fe}^{diffusion}$, mass of iron per unit surface area that diffuses into the bath, given by:

$$m_{Fe}^{diffusion} = m_{Fe}^{dissolved} - m_{Fe}^{coating} \quad (5)$$

The diffusion of iron into the bath can be seen to increase with rotation speed.

4.2. Variation of the bath composition

Fig. 4a and b show the variation of the iron and aluminium concentrations of the bath with cumulative galvanizing time, t_{total}, estimated using two methods: (1) analysis of bath samples (Section 3); and (2) calculation of the total mass of iron that has diffused into the bath and that of aluminium that has diffused to the steel surface (and is therefore present in the coating) during successive hot-dip galvanizing treatments.

The two measurement techniques give consistent results. For aluminium, the slight differences observed after one hour of cumulative galvanizing treatment can be explained by the formation of an alumina-rich film on the bath surface, which is skimmed off before each new specimen immersion. Only the bath samples take into account this secondary phenomenon of aluminium depletion in the bath.

The amount of iron in the liquid phase increases significantly with time (Fig. 4a). In order to exploit the experimental results, allowance must be made for the fact that dissolution of the steel substrate depends on the concentration of iron dissolved in the bath (Equation 1).

TABLE III Calculated errors due to the experimental procedure

Experimental step	Type of error	Error ($g.m^{-2}$)
1. Degreasing with chloroform	Reproducibility of the measurements (accuracy of the balance)	−0.1 to +0.1
2. Pickling	Variability of etching of the steel	−0.2 to −0.1
3. Fluxing	Initial surface more or less oxidised	−0.6 ± 0.2
4. Coating dissolution in HCl	Dissolution of the iron substrate or oxides reoxidation after leaving the solution	−0.1 ± 0.2

4.3. Calculation of the error on the weight measurements

The scatter of the experimental values of the mass of iron dissolved is $\pm 0.9\ g{\cdot}m^{-2}$. The uncertainty due to the experimental technique can be estimated by weighing without galvanizing (Table III). In the steps prior to galvanizing (1 to 3), the error determined after each step includes all those from previous steps and takes into account any possible compensation of certain errors. The uncertainty of the experimental measurements of the mass of iron dissolved is essentially associated with the fluxing step.

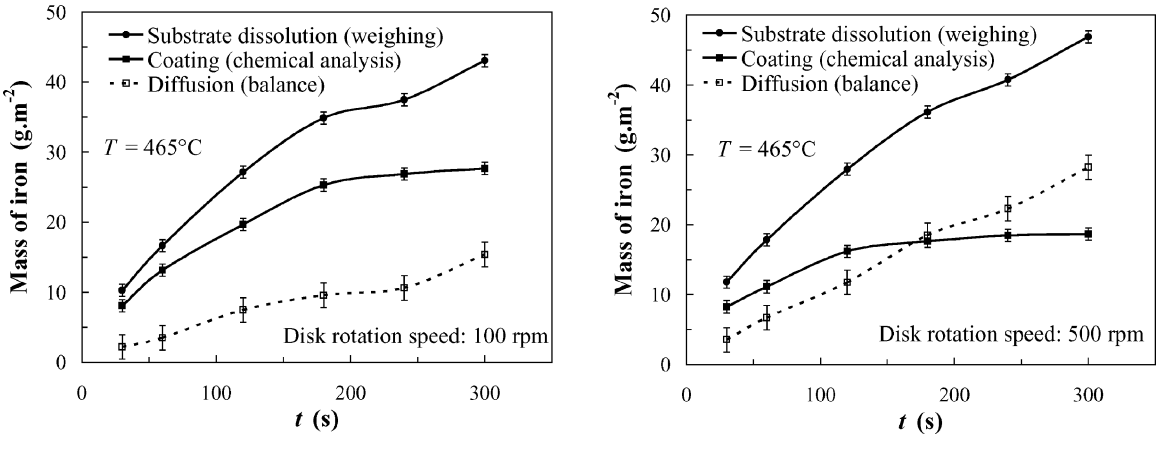

Figure 3 Iron matter balance as a function of immersion time for rotation speeds of 100 rpm (left) and 500 rpm (right).

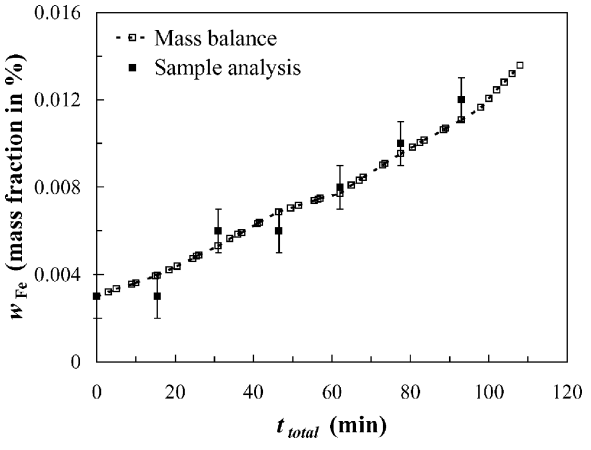

(a)

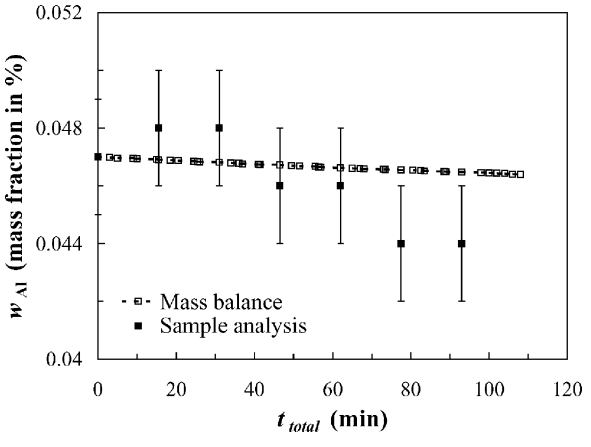

(b)

Figure 4 (a) Iron content of the bath. (b) Aluminium content of the bath.

5. Determination of the diffusion coefficient for iron in liquid zinc

5.1. Assumption concerning the iron dissolution law

In agreement with Equation 1, the iron dissolution reaction in the liquid is considered to be given by:

$$\frac{\mathrm{d}c_{\mathrm{Fe}}^{\infty}}{\mathrm{d}t} = k_{tot}\frac{S}{V}\left(c_{\mathrm{Fe}}^{sat} - c_{\mathrm{Fe}}^{\infty}\right) \tag{6}$$

where c_{Fe}^{∞} and c_{Fe}^{sat} are respectively the concentration of iron in the bath and the saturation value with respect to equilibrium with an iron-zinc compound (ζ [6] or δ [7]). Neglecting variations in the mass and volume of the bath, this gives:

$$\frac{\mathrm{d}w_{\mathrm{Fe}}^{\infty}}{\mathrm{d}t} = k_{tot}\frac{S}{V}\left(w_{\mathrm{Fe}}^{sat} - w_{\mathrm{Fe}}^{\infty}\right) \tag{7}$$

where w_{Fe}^{∞} and w_{Fe}^{sat} (=0.04 wt% at 465°C [6, 7]) are the mass fractions of iron in the bath and that at saturation.

Since the amount of iron in the liquid phase varies with time, this equation must be integrated for each specimen between the galvanizing times t_{total}^{i} and t_{total}^{i+1} (Fig. 4a):

$$\ln\left(\frac{w_{\mathrm{Fe}}^{sat} - w_{\mathrm{Fe}}^{\infty}\left(t_{total}^{i}\right)}{w_{\mathrm{Fe}}^{sat} - w_{\mathrm{Fe}}^{\infty}\left(t_{total}^{i+1}\right)}\right) = k_{tot}\frac{S}{V}\left(t_{total}^{i+1} - t_{total}^{i}\right) \tag{8}$$

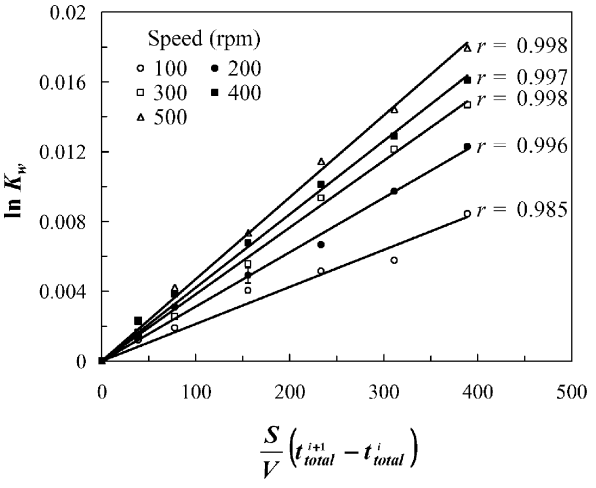

with $K_w = \left\{w_{\mathrm{Fe}}^{sat} - w_{\mathrm{Fe}}^{\infty}\left(t_{total}^{i}\right)\right\} / \left\{w_{\mathrm{Fe}}^{sat} - w_{\mathrm{Fe}}^{\infty}\left(t_{total}^{i+1}\right)\right\}$

Figure 5 Validation of the first order dissolution law.

5.2. Validation of the iron dissolution law

The relation

$$\ln\left(\frac{w_{\mathrm{Fe}}^{sat} - w_{\mathrm{Fe}}^{\infty}\left(t_{total}^{i}\right)}{w_{\mathrm{Fe}}^{sat} - w_{\mathrm{Fe}}^{\infty}\left(t_{total}^{i+1}\right)}\right) = f\left(\frac{S}{V}\left(t_{total}^{i+1} - t_{total}^{i}\right)\right) \tag{9}$$

is plotted for different rotation speeds in Fig. 5. Good straight line correlations are obtained (coefficient r close to 1), validating the proposed dissolution law. The slope determined by linear regression analysis is equal to the overall dissolution constant k_{tot}.

5.3. Diffusion coefficient of iron in liquid zinc

The overall dissolution constant k_{tot} varies linearly with the square root of the disk rotation speed (Fig. 6). This proves that, for the galvanizing conditions studied, the iron dissolution reaction is controlled by diffusion in the liquid phase. In all the experiments, laminar flow conditions prevailed ($8 \times 10^3 < \mathrm{Re} < 4 \times 10^4$). The diffusion coefficient for iron in liquid zinc at 465°C can be determined from Equation 3:

$$D_{\mathrm{Fe}}^{\mathrm{Zn(L)}} = (9.8 \pm 0.1) \times 10^{-10}\ \mathrm{m^2{\cdot}s^{-1}}$$
$$(\text{with Sc} \approx 510 \text{ and } f_{\mathrm{Sc}} \approx 0.928) \tag{10}$$

This value is close to that obtained by extrapolating to 465°C the measurements made by M. Kato and S. Minowa [19, 20] between 600 and 900°C. These authors brought into contact two zinc liquid phases containing different amounts of iron and determined the iron concentration profile established after a few hours (Equation 11, Fig. 7):

$$D_{\mathrm{Fe}}^{\mathrm{Zn(L)}} = 2 \times 10^{-7} \exp\left(-\frac{33600}{RT}\right) \quad (\mathrm{m^2{\cdot}s^{-1}}) \tag{11}$$

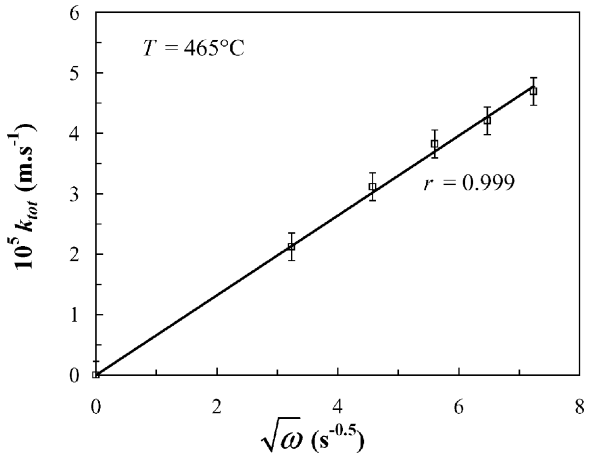

Figure 6 Variation of the overall dissolution constant k_{tot} with the square root of the rotation speed.

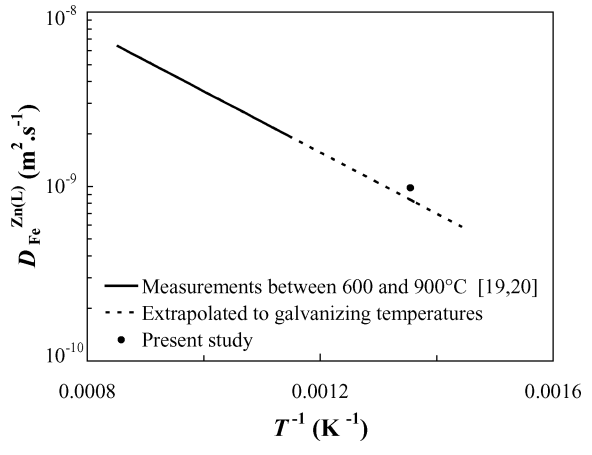

Figure 7 Comparison of the present result with data from the literature.

6. Conclusions and future prospects

Experiments using the rotating disk technique have demonstrated that the dissolution of iron in liquid zinc containing only small amounts of aluminium (0.05 wt%) and iron (0.003 wt%) is controlled by the diffusion of iron in the liquid phase. The method involves monitoring the dissolution of iron from steel disks, by weighing and chemical analysis, as a function of immersion time and disk rotation speed. The diffusion coefficient of iron in liquid zinc determined in this way is:

$$D_{\mathrm{Fe}}^{\mathrm{Zn(L)}} = (9.8 \pm 0.1) \times 10^{-10}\ \mathrm{m^2 \cdot s^{-1}}$$

This diffusion coefficient is a key parameter for the hot-dip galvanizing of steels, since it determines the flux of dissolved iron from the strip that diffuses into the zinc bath. This is important for improved bath management, enabling quantification of the exchanges of iron between the steel and the liquid zinc. This information cannot be obtained directly during the industrial process and is accessible only by modelling the kinetics of the galvanizing reactions [22]. The iron diffusion coefficient measured in the present study is an essential parameter for modelling.

Acknowledgements

The authors are extremely grateful to Dr. M. Guttmann for his enthusiasm and help with this study and extend their thanks to the staff of the IRSID analytical chemistry laboratory for their valuable assistance.

References

1. D. HORSTMANN, "Reactions between Iron and Molten Zinc" (Zinc Development Association, London, 1978) p. 1.
2. M. GUTTMANN, *Mat. Sci. Forum* **155/156** (1994) 527.
3. A. R. MARDER, *Prog. Mater. Sci.* **45**(3) (2000) 191.
4. S. YAMAGUCHI, in Proceedings of the 4th International Conference on Zinc and Zinc Alloy Coated Steel Sheet (Galvatech'98), Chiba, Japan, Sept. 1998 (The Iron and Steel Institute of Japan, Tokyo, 1998) p. 84.
5. O. KUBASCHEWSKI, "Iron Binary Phase Diagrams" (Springer-Verlag, Berlin, 1982) p. 5.
6. N.-Y. TANG, *J. Phase Equilibria* **21**(1) (2000) 70.
7. J. R. MCDERMID and W. T. THOMSON, in Proceedings of the 44th Mechanical Working and Steel Processing (MWSP) Conference, Sept. 2002 (Iron and Steel Society, Warrendale, 2002) Vol. **XL**, p. 805.
8. V. G. LEVICH, "Physicochemical Hydrodynamics" (Prentice-Hall, Inc., Englewood Cliffs, N.J., 1962) p. 60.
9. T. F. KASSNER, *J. Electrochem. Soc.* **114**(7) (1967) 689.
10. V. N. YEREMENKO, YA. V. NATANZON and V. I. DYBKOV, *J. Less-Common Met.* **50**(1) (1976) 29.
11. *Idem*, *J. Mater. Sci.* **16** (1981) 1748.
12. S. K. CHUCHMAREV, V. I. POKHMURSKII, YU. A. RAEVSKII, YU. G. DMITRIEV and O. YA. LIZUN, *Sov. Mater. Sci. (English Translation of Fiz.-Him. Mek. Mater.)* **21**(5) (1985) 17.
13. V. I. DYBKOV, *J. Mater. Sci.* **25**(8) (1990) 3615.
14. YA. V. NATANZON, V. P. TITOV and R. V. ANTONCHENKO, *Sov. Powder Metall. Met. Ceram. (English Translation of Porosk. Metall.)* **2**(350) (1992) 73.
15. V. I. DYBKOV, *J. Mater. Sci.* **28**(23) (1993) 6371.
16. A. A. HERSHMAN, in Proceedings of the 7th International Conference on Hot Dip Galvanizing, Paris, June 1964 (Pergamon Press, Oxford, 1967) p. 189.
17. H. YAMAGUCHI and Y. HISAMATSU, *Tetsu-to-Hagané* **59**(1) (1973) 131.
18. H. KOGA, Y. UCHIYAMA and T. AKI, *Trans. Jpn. Inst. Met.* **20**(6) (1979) 290.
19. M. KATO and S. MINOWA, *Tetsu-to-Hagané* **50**(12) (1964) 2083.
20. *Idem.*, *ibid.* **52**(1) (1966) 32.
21. L.-D. LUCAS, "Techniques de l'Ingénieur, Traité des Matériaux Métalliques MI" (Éditions Techniques de l'Ingénieur, Paris, 1996) Vol. M65, p. 1 (in French).
22. M.-L. GIORGI, "Studies on the Kinetics of Galvanizing Reactions", Ph.D. Thesis, Ecole Centrale Paris, May 2000 (in French).

Received 10 July 2003
and accepted 6 May 2004